

# Ergodicity of One-dimensional Systems Coupled to the Logistic Thermostat

Diego Tapias<sup>1</sup>, Alessandro Bravetti<sup>2</sup>, David P. Sanders<sup>3,4</sup>

<sup>1</sup>*Departamento de Física, Facultad de Ciencias, Universidad Nacional Autónoma de México  
Ciudad Universitaria, Ciudad de México 04510, México  
E-mail: diego.tapias@nucleares.unam.mx*

<sup>2</sup>*Instituto de Investigaciones en Matemáticas Aplicadas y en Sistemas, Universidad Nacional Autónoma de México,  
Ciudad Universitaria, Ciudad de México 04510, México  
E-mail: alessandro.bravetti@iimas.unam.mx*

<sup>3</sup>*Departamento de Física, Facultad de Ciencias, Universidad Nacional Autónoma de México  
Ciudad Universitaria, Ciudad de México 04510, México  
E-mail: dpsanders@ciencias.unam.mx*

<sup>4</sup>*Computer Science and Artificial Intelligence Laboratory, Massachusetts Institute of Technology  
77 Massachusetts Avenue, Cambridge, MA 02139, USA*

Received: 04 December 2016; revised: 10 January 2017; accepted: 11 January 2017; published online: 31 January 2017

**Abstract:** We analyze the ergodicity of three one-dimensional Hamiltonian systems, with harmonic, quartic and Mexican-hat potentials, coupled to the logistic thermostat. As criteria for ergodicity we employ: the independence of the Lyapunov spectrum with respect to initial conditions; the absence of visual “holes” in two-dimensional Poincaré sections; the agreement between the histograms in each variable and the theoretical marginal distributions; and the convergence of the global joint distribution to the theoretical one, as measured by the Hellinger distance. Taking a large number of random initial conditions, for certain parameter values of the thermostat we find no indication of regular trajectories and show that the time distribution converges to the ensemble one for an arbitrarily long trajectory for all the systems considered. Our results thus provide a robust numerical indication that the logistic thermostat can serve as a single one-parameter thermostat for stiff one-dimensional systems.

**Key words:** logistic thermostat, ergodicity, Gibbs’ ensemble

## I. INTRODUCTION

The introduction by Nosé and Hoover of deterministic equations of motion consistent with the canonical ensemble allowed to make a connection between microscopic and macroscopic descriptions for ensembles different from the microcanonical [1, 2]. However, there is a practical limitation that impedes the use of the Nosé-Hoover equations for a given system, namely ergodicity. Roughly speaking, a system is *ergodic* if for almost any trajectory, taking long-time averages is equivalent to taking ensemble averages [3, 4]. For the majority of physical systems, ergodicity can be tested only through numerical experiments.

The Nosé-Hoover thermostat fails to be ergodic for a one-dimensional harmonic oscillator [2]. Therefore, various alternative schemes have been proposed to simulate a harmonic oscillator in the canonical ensemble [5-11], some of which seem to be ergodic, in the sense that they pass a series of different numerical tests designed to detect this property. Among the ergodic schemes, the “0532” thermostat is the only one that requires the addition of a single thermostating force [11] (see also the discussion in [12]).

The “0532” model was inspired by the observation that a cubic thermostat force enhances ergodicity with respect to the linear (Nosé-Hoover) one [5, 6, 11]. Thus the authors

in [11] started with a general parametric three-dimensional dynamical system with a cubic friction force, designed to control directly the first three even moments of the momentum  $p$ . They then adjusted the parameters for the case of a harmonic potential, using a  $\chi^2$  test, by imposing that the joint probability distribution be Gaussian in the three variables.

The method described in the last paragraph can be extended in principle to more general one-dimensional potentials. However, there are two major drawbacks. First, one has to repeat the  $\chi^2$  test for each potential, which is a computationally demanding task. Second, the form of the parametric equations to be tested may depend on the potential of the system to be thermostatted and thus the idea of generality behind the Nosé-Hoover equations is lost. Furthermore, the analysis in [13] has shown that this thermostat works well for the one-dimensional harmonic oscillator, but not for the quartic potential.

For these reasons it is relevant to ask if there is a general scheme depending just on the addition of a single thermostating force that allows the generation of a large family of ergodic singly-thermostatted one-dimensional systems (STIDS). This is the challenge of the 2016 Ian Snook prize [13] and the subject of this work.

We start from an algorithm to generate the equations of motion known as Density Dynamics [14]. Combining this scheme with the *logistic thermostat* introduced previously [15, 16] by two of the present authors, we generate a set of STIDS for different potentials and we show that such systems pass all the numerical tests for ergodicity. The advantage of the Density Dynamics formalism is that the equations of motion are the same in form for any Hamiltonian system, thus retaining the spirit of generality of Nosé and Hoover [14]. The superiority of the logistic thermostat comes from the fact that the thermostating force is highly nonlinear, thus enhancing the ergodicity of the dynamics. Additionally, we show that the equations of motion that we obtain are time-reversible. All these aspects make the logistic thermostat appealing from both a practical and a theoretical perspective.

The structure of the paper is as follows. In section II., we give an introduction to the Density Dynamics formalism and present the logistic thermostat. In section III., we present the numerical methods used to study ergodicity, together with the results obtained. Finally, in section IV. we summarize our results and present the conclusions.

## II. DENSITY DYNAMICS

The Density Dynamics (DD) method was introduced by Fukuda and Nakamura, inspired by the Nosé-Hoover equations of motion [14]. Afterwards, the same method was re-derived by Bravetti and Tapias, starting from a dynamics based on a generalization of Hamilton's equations [15-17].

The DD method provides an algorithm for the generation of a set of equations in a  $(2n + 1)$ -dimensional space consis-

tent with a prescribed probability distribution ( $n$  being the degrees of freedom of the physical system). For a general description of the method we refer to [14-16]. In this section we present its application to STIDS.

Let  $n = 1$  and consider the 3-dimensional extended phase space with coordinates  $(q, p, \zeta)$ . A one-dimensional Hamiltonian system coupled to a thermostat is expected to present a canonical probability distribution in  $(q, p)$ . So, the invariant distribution to be generated in  $(q, p, \zeta)$  is of the form

$$\rho(q, p, \zeta) = \frac{e^{-\beta H(q, p)}}{\mathcal{Z}} f(\zeta), \quad (1)$$

where  $\mathcal{Z}$  is a normalization constant and  $f(\zeta)$  is a 1-dimensional probability distribution in  $\zeta$ , i.e.  $f(\zeta)$  is a strictly positive, smooth, integrable function with support in  $\mathbb{R}$ . According to the DD prescription, the equations of motion consistent with the probability density (1) are

$$\dot{q} = \frac{\partial H(q, p)}{\partial p}, \quad (2)$$

$$\dot{p} = -\frac{\partial H(q, p)}{\partial q} + \frac{f'(\zeta)}{\beta f(\zeta)} p, \quad (3)$$

$$\dot{\zeta} = \frac{\partial H(q, p)}{\partial p} p - \frac{1}{\beta}. \quad (4)$$

Consistency between the field  $v = (\dot{q}, \dot{p}, \dot{\zeta})$  and the distribution (1) means that the Liouville equation is satisfied for this pair, i.e.

$$\begin{aligned} \text{div}(\rho v) &= \nabla \cdot (\rho v) = (\nabla \rho) \cdot v + \rho (\nabla \cdot v) = \\ &= \frac{\partial \rho}{\partial q} \dot{q} + \frac{\partial \rho}{\partial p} \dot{p} + \frac{\partial \rho}{\partial \zeta} \dot{\zeta} + \rho \left( \frac{\partial \dot{q}}{\partial q} + \frac{\partial \dot{p}}{\partial p} + \frac{\partial \dot{\zeta}}{\partial \zeta} \right) \\ &= \rho \left( -\beta \frac{\partial H}{\partial q} \frac{\partial H}{\partial p} - \beta \frac{\partial H}{\partial p} \left( -\frac{\partial H}{\partial q} \right. \right. \\ &\quad \left. \left. + \frac{f'}{\beta f} p \right) + \frac{f'}{f} \left( \frac{\partial H}{\partial p} p - \frac{1}{\beta} \right) \right) \\ &\quad + \rho \left( \frac{\partial^2 H}{\partial p \partial q} - \frac{\partial^2 H}{\partial q \partial p} + \frac{f'}{\beta f} \right) = 0. \end{aligned} \quad (5)$$

Naturally, this proof extends directly to systems with more degrees of freedom.

### II. 1. The logistic thermostat

The set of equations (2)-(4) depends on the probability distribution chosen for the extended variable  $f(\zeta)$ , associated with the effect of the thermal reservoir. By choosing a Gaussian distribution with variance  $Q$  and mean 0, we recover the time-reversible Nosé-Hoover equations of motion. These dynamical equations modify the structure of Hamilton's equations by adding a linear friction term that obeys a feedback equation that controls the kinetic energy [2]. For the same system, one can consider different distributions  $f(\zeta)$ . For instance, a Gaussian distribution for  $\zeta^2$  introduces

a cubic friction term, which considerably improves ergodicity [5, 14, 18].

Following the observation that nonlinearity enhances ergodicity, we choose  $f(\zeta)$  to be a logistic distribution:

$$f_{\text{logistic}}(\zeta) = \frac{e^{\frac{\zeta-\mu}{Q}}}{Q(1+e^{\frac{\zeta-\mu}{Q}})^2} = \frac{1}{4Q} \text{sech}^2\left(\frac{\zeta-\mu}{2Q}\right), \quad (6)$$

where  $\mu$  is the mean of the distribution and the variance is  $Q^2\pi^2/3$ . We call this choice the *logistic thermostat* and refer to  $Q$  as the “mass” associated with the thermostat, using the same terminology as for the Nosé-Hoover case [19].

In our previous works we used the logistic thermostat with the choice of the parameters  $Q = 1$  and  $\mu = 2$  and we showed that this is a suitable choice to perform molecular dynamics simulations [15, 16]. However, these particular values make the resulting dynamical system not time-reversible, which is an important property for a dynamical model that aims to simulate equilibrium. Here we fix this issue by suggesting a different parameter choice. Choosing  $\mu = 0$ , we see that  $f(\zeta)$  becomes an even function and it follows that the corresponding equations of motion

$$\dot{q} = \frac{\partial H(q, p)}{\partial p}, \quad (7)$$

$$\dot{p} = -\frac{\partial H(q, p)}{\partial q} - \frac{\tanh\left(\frac{\zeta}{2Q}\right)}{\beta Q} p, \quad (8)$$

$$\dot{\zeta} = \frac{\partial H(q, p)}{\partial p} p - \frac{1}{\beta} \quad (9)$$

are time-reversible, i.e. invariant under the transformation  $(q, p, \zeta, t) \rightarrow (q, -p, -\zeta, -t)$ . Equations (7)-(9) constitute our system that provides thermostatted dynamics for any one-dimensional Hamiltonian system encoded in  $H(q, p)$ .

### III. NUMERICAL TESTS AND RESULTS

In this section we numerically test the ergodicity of the system (7)-(9) for three Hamiltonian systems with Hamiltonians given by

$$H(p, q) = \frac{p^2}{2} + V(q), \quad (10)$$

with potentials

- $V(q) = q^2/2$  (harmonic);
- $V(q) = q^4/4$  (quartic);
- $V(q) = -q^2/2 + q^4/4$  (Mexican hat).

Throughout this section the (inverse) temperature is taken as  $\beta = 1.0$ . The “mass” of the thermostat for the harmonic and quartic systems is  $Q = 0.1$ , whereas for the Mexican hat potential it is  $Q = 0.02$ . These values were chosen on the base of preliminary tests designed to detect violations of ergodicity. For instance, for  $Q = 0.1$  in the case of the Mexican hat potential we found 5 regular trajectories out of 1 million

initial conditions, thus indicating a violation of ergodicity. For this reason the value of  $Q$  considered for such potential is different from the one used for the other systems.

Before proceeding with the numerical analysis, we summarize the relationship between such tests and ergodicity. In essence, an ergodic thermostatted system is expected to present a single chaotic sea of full measure in its extended phase space, so that for almost any initial condition in this set, the numerical distribution in time converges to the theoretical distribution in the ensemble [9, 20, 21]. The study of the chaotic sea relies on both the analysis of the Lyapunov spectrum for a large number of initial conditions and on the observation of Poincaré sections. With these tests one checks the independence of the spectrum with respect to the initial condition and discards the presence of islands that would violate the assumption that the chaotic sea has full measure. Then one proceeds to analyse the equivalence between the numerical distribution and the theoretical one. For this, one observes the visual agreement between the numerical histograms and the marginal theoretical distributions and checks the mean values of certain observables [5, 7, 14, 22]. Recently, stronger tests have been used to analyze the convergence between distributions, based on distances in the distributions space [23, 24]. Here we consider the Hellinger distance [24, 25].

#### III. 1. Lyapunov characteristic exponents

For a dynamical system, the Lyapunov characteristic exponents (LCEs) are asymptotic measures characterizing the average rate of growth (or shrinking) of small perturbations of the solutions [26]. The set of LCEs is grouped in the Lyapunov spectrum.

There are three facts about the Lyapunov spectrum that are relevant for our numerical study: if the largest exponent in the spectrum for a given trajectory is greater than zero, then the trajectory is chaotic; if the sum of exponents in the spectrum for a given trajectory is equal to zero, then its nearby volume is maintained on average; finally, if the spectrum is independent of the initial condition, then the system is ergodic.

In the following, we report the numerical conditions used and discuss our results; for a similar study for different thermostat models, see Ref. [21]. We take ten thousand random initial conditions for each system, with a weight given by the logistic distribution in  $\zeta$  with mean  $\mu = 0$  and  $Q$  chosen according to the potential, as specified above, and by the normal distribution in  $p$  and  $q$ , with mean 0 and variance 1 for each variable. We follow the procedure of Bennetin et al. [26, 27] to calculate the Lyapunov spectrum by setting up the variational equations associated with the system (7)-(9) and solving them together with the original system for each initial condition, using a fourth-order Runge-Kutta integrator with a step size of 0.005 and  $10^7$  time steps.

The relevant results regarding the Lyapunov spectra for each case are reported in Tab. 1. With this test we deduce

	$\lambda_1$	$\lambda_2$	$\lambda_3$
Harmonic	$0.281 \pm 2 \times 10^{-3}$	$0.000 \pm 3 \times 10^{-5}$	$-0.281 \pm 2 \times 10^{-3}$
Quartic	$0.243 \pm 2 \times 10^{-3}$	$0.000 \pm 4 \times 10^{-5}$	$-0.243 \pm 2 \times 10^{-3}$
Mexican hat	$0.385 \pm 7 \times 10^{-3}$	$0.000 \pm 7 \times 10^{-3}$	$-0.386 \pm 7 \times 10^{-3}$

Tab. 1. Mean Lyapunov characteristic exponents, estimated with 10000 different random initial conditions. The errors are standard deviations

that the systems are chaotic and that the exponents within each spectrum add to zero, thus characterizing an equilibrium system (zero average contraction of volume in the extended phase space). Furthermore, the small relative value of the standard deviation suggests the independence of the spectra with respect to the initial condition.

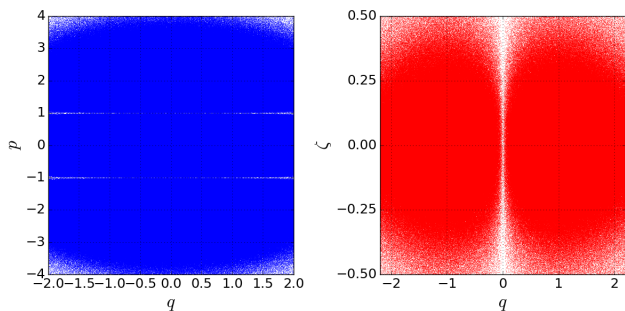


Fig. 1. Poincaré sections for the harmonic potential. Around  $3 \times 10^7$  crossings are shown for the section  $\zeta = 0$  (left) and  $3 \times 10^6$  crossings for the section  $p = 0$  (right). Additionally, the nullcline lines  $p = \pm 1$  (left) and  $q = 0$  (right) are observed

We now proceed to analyze in depth this property. For that, we consider one million initial conditions and integrate the equations of motion needed to obtain the largest LCE for a short time, but sufficiently long to discriminate between a regular and a chaotic trajectory, which we estimate as 500 times the Lyapunov time (inverse of the largest Lyapunov exponent [26]). Then we check the consistency between the exponent obtained and the expected one as given in Tab. 1. When a possible regular trajectory is detected via an anomalously low value of the largest Lyapunov exponent, the equations are integrated for a longer time. We find that for the three systems considered the spectrum is independent of the initial condition.

### III. 2. Poincaré sections

The second test of ergodicity is based on Poincaré sections for a very long trajectory. The visual observation of “holes” in these sections is an indication of the lack of ergodicity [18].

We pick a random initial condition (weighted as in the previous subsection) and integrate numerically the equations (7)-(9) using the adaptive Dormand-Prince Runge-Kutta (4-5) integrator up to a total time of  $1.25 \times 10^7$ . Then we choose two cross sections, given by  $\zeta = 0$  and  $p = 0$  respectively,

and record a point each time the section is crossed. In this way we construct the figures 1, 2 and 3.

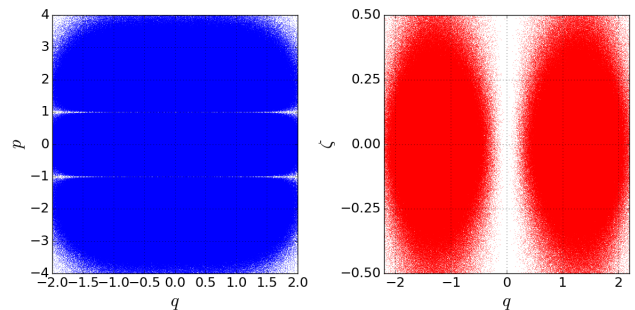


Fig. 2. Poincaré sections for the quartic potential.  $3 \times 10^7$  crossings are shown for the section  $\zeta = 0$  (left) and  $3 \times 10^6$  crossings for the section  $p = 0$  (right). Additionally, the nullcline lines  $p = \pm 1$  (left) and  $q = 0$  (right) are observed

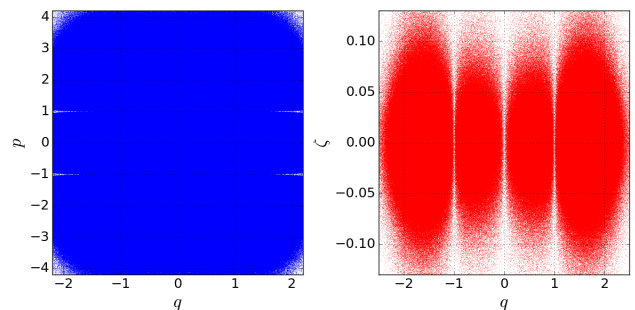


Fig. 3. Poincaré sections for the Mexican hat potential. Around  $1 \times 10^8$  crossings are shown for the section  $\zeta = 0$  (left) and  $4 \times 10^6$  crossings for the section  $p = 0$  (right). Additionally, the nullcline lines  $p = \pm 1$  (left) and  $q = 0, \pm 1$  (right) are observed

We visually observe the absence of “holes” in the cross sections, which constitutes an additional indication of ergodicity.

### III. 3. Marginal distributions

Having determined the existence of the chaotic sea, we proceed to analyze the relation between the distributions. In figures 4, 5 and 6 we check that the numerical marginal distributions correspond to the theoretical ones. In the next section we provide a stronger test, which confirms the convergence of the joint distribution.

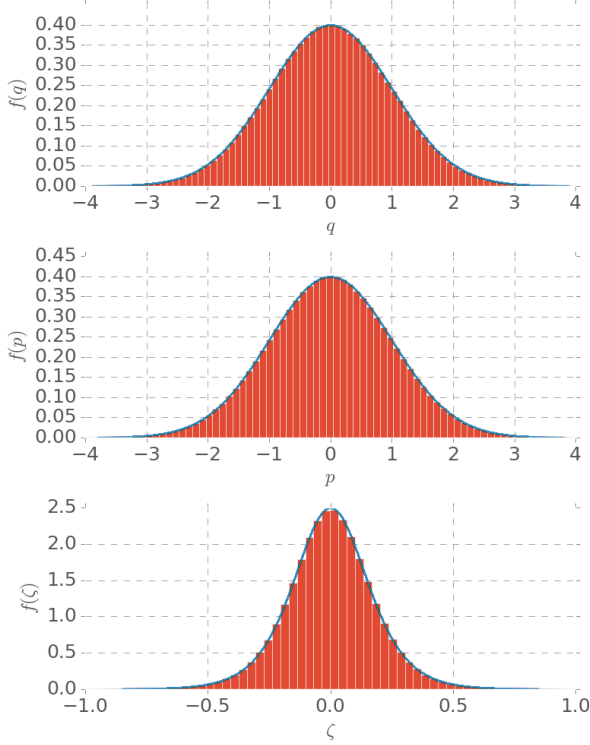


Fig. 4. Histograms compared with exact marginal distributions (solid line) for the harmonic potential

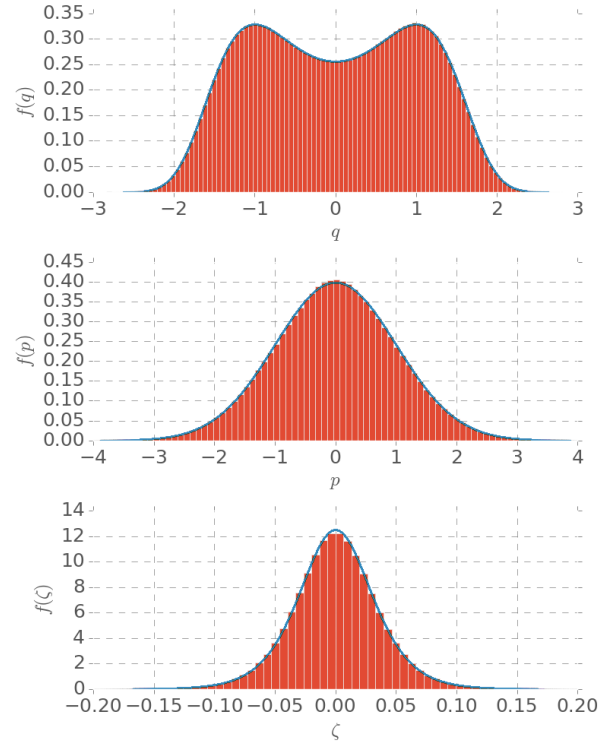


Fig. 6. Histograms compared with exact marginal distributions (solid line) for the Mexican hat potential

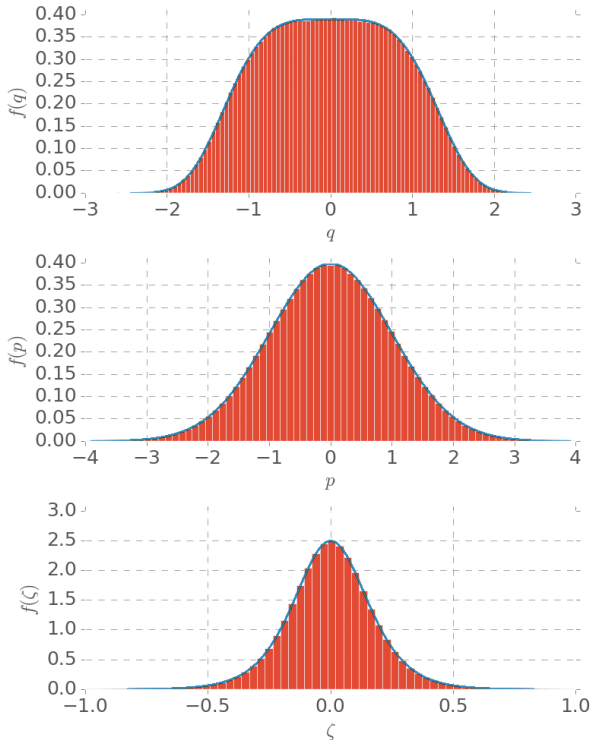


Fig. 5. Histograms compared with exact marginal distributions (solid line) for the quartic potential

### III. 4. Hellinger distance

The DD formalism, by construction, predicts that the joint invariant probability density is (1), where in our case  $f(\zeta)$  is given by (6) and  $\mu = 0$ . Explicitly, we have

$$\rho(p, q, \zeta; Q) = \frac{e^{-\beta H(q, p)} \operatorname{sech}^2\left(\frac{\zeta}{2Q}\right)}{\mathcal{Z} 4Q} \quad (11)$$

In this section we analyze the convergence of the numerical joint distribution associated with a very long trajectory to the theoretical invariant distribution (11). For the comparison we use a measure of distance between distributions, the Hellinger distance, which in the extended phase space is defined as [25]

$$D_H(g||f) = 2 \int \int \int \left( \sqrt{g} - \sqrt{f} \right)^2 dq dp d\zeta, \quad (12)$$

where  $f$  and  $g$  are two three-variate distributions. To calculate this distance, we again integrate a random initial condition with the Dormand-Prince Runge-Kutta (4-5) integrator for a total time  $t = 1.25 \times 10^6$  and sample  $q, p, \zeta$  at a uniform time  $dt_{\text{sampling}} = 0.125$ . For each time interval we determine the experimental joint density by using the Kernel Density Estimation method [25] and then we integrate numerically the equation (12) by considering  $g$  as the experimental density and  $f$  the theoretical one (11). The domain of integration corresponds to the smallest rectangular domain in the extended phase space that contains the whole region explored by the

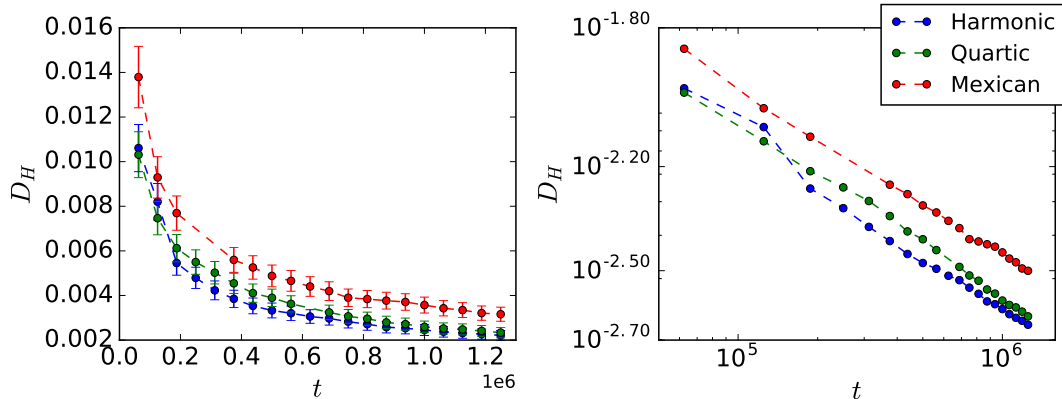


Fig. 7. Hellinger distance for the three potentials as a function of integration time. The right panel shows the log-log plot

trajectory. The results of the evolution of the Hellinger distance with time are displayed in figure 7. As the figure reveals, there is a convergence to the expected distribution with time in all three cases. This completes our study of ergodicity for the potentials considered.

Finally, in order to check that our results do not depend on the integration scheme, we have also performed the simulations using the geometric integrator for systems in the canonical ensemble that we have proposed in [16]. All the tests give the same results, thus confirming that they are independent of the choice of the integrator.

#### IV. CONCLUSIONS

In this work we have performed a thorough numerical investigation on the ergodicity of three important singly-thermostatted one-dimensional systems. We employed a logistic thermostat within the context of the Density Dynamics formalism, with the corresponding equations of motion being a set of coupled time-reversible differential equations, see (7)-(9). These equations have the same structure as those of Nosé-Hoover, but they differ in the friction term, being linear in the Nosé-Hoover case and highly non-linear in our (logistic) case.

For the one-dimensional Hamiltonian systems studied, with a quadratic, quartic and Mexican hat potentials, we numerically studied their ergodicity using four tests:

- Independence of the Lyapunov spectrum from the initial condition.
- No visual holes in the Poincaré sections.
- Agreement between marginal distributions and numerical frequencies.
- Convergence of the joint numerical distribution to the theoretical one, quantified by the Hellinger distance.

All the systems considered passed these numerical tests for ergodicity, thus providing strong numerical evidence that the dynamics of the logistic thermostat with suitable param-

eter values is ergodic for such systems. The programs used for the simulations, written in the Julia language, are available at [28]. Our results show the relevance of the Density Dynamics formalism as a method to generate dynamics compatible with an arbitrary probability distribution. Additionally, we remark the superiority of the logistic thermostat to enhance ergodicity with respect to other thermostats previously used in this framework [9].

In future work, we plan to explore in depth the structure of the phase space as the parameters  $Q$  and  $\beta$  are varied. As the STIDS are time-reversible dynamical systems, they present characteristics which are very similar to those of Hamiltonian systems (e.g. periodic orbits, tori, stochastic regions, etc.) [29, 30]. This structure has been analyzed, for instance, for the harmonic oscillator coupled to the Nosé-Hoover thermostat, showing very interesting properties [31-33]. An analysis of this kind may help to understand the nature of the ergodic behaviour displayed for the parameters chosen in this work.

Additionally, it would be a challenging task to consider a theoretical approach to ergodicity of thermostatted systems by exploiting its geometric structure, as has been done for hamiltonian systems [34].

#### Acknowledgements

The authors would like to thank Prof. Hoover and Prof. Fukuda for their stimulating comments and Edison Montoya and Uriel Aceves for technical and computational support. AB is supported by a DGAPA-UNAM postdoctoral fellowship. DT acknowledges financial support from CONACYT, CVU No. 442828. DPS acknowledges financial support from DGAPA-UNAM grant PAPIIT-IN117214, and from a CONACYT sabbatical fellowship, and thanks Alan Edelman and the Julia group at MIT for hospitality while this work was carried out.

## References

- [1] S. Nosé, *A molecular dynamics method for simulations in the canonical ensemble*, Molecular Physics **52**, 255-268 (1984).
- [2] W. G. Hoover, *Canonical dynamics: equilibrium phase-space distributions*, Physical Review A **31**(3), 1695 (1985).
- [3] C.R. de Oliveira, T. Werlang, *Ergodic hypothesis in classical statistical mechanics*, Revista Brasileira de Ensino de Física **29**(2), 189-201, (2007).
- [4] I. Aleksandr, A. Khinchin, *Mathematical foundations of statistical mechanics*, Courier Corporation, 1949.
- [5] D. Kusnezov, A. Bulgac, W. Bauer, *Canonical ensembles from chaos*, Annals of Physics **204**(1), 155-185 (1990).
- [6] D. Kusnezov, A. Bulgac, *Canonical ensembles from chaos II: Constrained dynamical systems*, Annals of Physics **214**(1), 180-218 (1992).
- [7] G.J. Martyna, M.L. Klein, M. Tuckerman, *Nosé-Hoover chains: The canonical ensemble via continuous dynamics*, The Journal of Chemical Physics **97**(4), 2635-2643 (1992).
- [8] Wm.G. Hoover, B.L. Holian, *Kinetic moments method for the canonical ensemble distribution*, Physics Letters A **211**(5), 253-257 (1996).
- [9] A.C. Brañka, M. Kowalik, K.W. Wojciechowski, *Generalization of the Nosé-Hoover approach*, The Journal of Chemical Physics **119**(4), 1929-1936 (2003).
- [10] A. Sergi, G.S. Ezra, *Bulgac-Kusnezov-Nosé-Hoover thermostats*, Physical Review E **81**(3), 036705 (2010).
- [11] Wm.G. Hoover, C.G. Hoover, J. Clinton Sprott, *Nonequilibrium systems: hard disks and harmonic oscillators near and far from equilibrium*, Molecular Simulation **42**(16), 1300-1316 (2016).
- [12] J.D. Ramshaw, *General formalism for singly thermostated Hamiltonian dynamics*, Physical Review E **92**(5), 052138 (2015).
- [13] Wm.G. Hoover, C.G. Hoover, *Singly-Thermostated Ergodicity in Gibbs' Canonical Ensemble and the 2016 Ian Snook Prize*, arXiv preprint arXiv:1607.04595 (2016).
- [14] I. Fukuda, H. Nakamura, *Tsallis dynamics using the Nosé-Hoover approach*, Physical Review E **65**(2), 026105 (2002).
- [15] A. Bravetti and D. Tapias, *Thermostat algorithm for generating target ensembles*, Physical Review E **93**, 022139 (2016).
- [16] D. Tapias, D.P. Sanders, A. Bravetti, *Geometric integrator for simulations in the canonical ensemble*, The Journal of Chemical Physics **145**(8) (2016).
- [17] A. Bravetti and D. Tapias, *Liouville's theorem and the canonical measure for nonconservative systems from contact geometry*, Journal of Physics A: Mathematical and Theoretical **48**(24), 245001 (2015).
- [18] Wm.G. Hoover, J. Clinton Sprott, C.G. Hoover, *Ergodicity of a singly-thermostated harmonic oscillator*, Communications in Nonlinear Science and Numerical Simulation **32**, 234-240 (2016).
- [19] P.H. Hünenberger, *Thermostat algorithms for molecular dynamics simulations*, In *Advanced computer simulation*, pages 105-149 Springer, 2005.
- [20] P.K. Patra, B. Bhattacharya, *An ergodic configurational thermostat using selective control of higher order temperatures*, The Journal of Chemical Physics **142**(19), 194103 (2015).
- [21] P.K. Patra, J. Clinton Sprott, Wm.G. Hoover, C.G. Hoover, *Deterministic time-reversible thermostats: chaos, ergodicity, and the zeroth law of thermodynamics*, Molecular Physics **113**(17-18), 2863-2872 (2015).
- [22] B. Leimkuhler, *Generalized Bulgac-Kusnezov methods for sampling of the Gibbs-Boltzmann measure*, Physical Review E **81**(2), 026703 (2010).
- [23] B. Leimkuhler, E. Noorizadeh, F. Theil, *A gentle stochastic thermostat for molecular dynamics*, Journal of Statistical Physics **135**(2), 261-277 (2009).
- [24] P.K. Patra, B. Bhattacharya, *Nonergodicity of the Nosé-Hoover chain thermostat in computationally achievable time*, Physical Review E **90**(4), 043304 (2014).
- [25] A. Basu, H. Shioya, C. Park, *Statistical inference: the minimum distance approach*, CRC Press, 2011.
- [26] Ch. Skokos, *The Lyapunov characteristic exponents and their computation*, In *Dynamics of Small Solar System Bodies and Exoplanets*, pages 63-135 Springer, 2010.
- [27] G. Benettin, L. Galgani, A. Giorgilli, J.M. Strelcyn, *Lyapunov characteristic exponents for smooth dynamical systems and for Hamiltonian systems: A method for computing all of them*, Meccanica **15**(9) (1980).
- [28] <https://github.com/dapias/ThermostattedDynamics.jl>.
- [29] J.A.G. Roberts, G.R.W. Quispel, *Chaos and time-reversal symmetry. Order and chaos in reversible dynamical systems*, Physics Reports **216**(2), 63-177 (1992).
- [30] J.S.W. Lamb, J.A.G. Roberts, *Time-reversal symmetry in dynamical systems: a survey*, Physica D: Nonlinear Phenomena **112**(1), 1-39 (1998).
- [31] H.A. Posch, Wm.G. Hoover, F.J. Vesely, *Canonical dynamics of the Nosé oscillator: stability, order, and chaos*, Physical Review A **33**(6), 4253 (1986).
- [32] L. Wang, X.-S. Yang, *The invariant tori of knot type and the interlinked invariant tori in the Nosé-Hoover oscillator*, The European Physical Journal B **88**(3), 1-5 (2015).
- [33] L. Wang, X.-S. Yang, *A vast amount of various invariant tori in the Nosé-Hoover oscillator*, Chaos: An Interdisciplinary Journal of Nonlinear Science **25**(12), 123110 (2015).
- [34] C. Liverani, M.P. Wojtkowski, *Ergodicity in Hamiltonian systems*, In *Dynamics reported*, pages 130-202 Springer, 1995.





**Diego Tapias** received his Bachelor of Science in Chemistry from the National University of Colombia in 2011 and his MSc from the National Autonomous University of Mexico (UNAM) in 2013. Currently he is a PhD candidate at the UNAM. His research focuses on algorithms for molecular dynamics, a differential geometric approach to the description of dissipative systems and the foundations of statistical mechanics.



**Alessandro Bravetti** received his MSc in Mathematics from the University of Camerino (Italy) in 2009 and his PhD in Relativistic Astrophysics from the University of Rome “Sapienza” in 2014. Currently he is a Postdoctoral researcher at the Instituto de Investigaciones en Matemáticas Aplicadas y en Sistemas (IIMAS) of the National Autonomous University of Mexico (UNAM). He is working on mathematical physics, with interests including the application of differential geometry to dissipative systems, information geometry, black hole physics and the foundations of statistical mechanics and thermodynamics.



**David P. Sanders** is Associate Professor at the Department of Physics of the Faculty of Sciences at the National Autonomous University of Mexico (UNAM). He received his PhD in Applied Mathematics from the University of Warwick, UK, in 2005. His research interests are in dynamical systems and statistical physics, with a focus on computational approaches. Topics he has worked on include billiard models, random walks, metastability, Markov Chain Monte Carlo, and thermostated dynamics. Recently, he has developed an interest in validated numerical methods.